Structural Analysis of a Sampling of Tesserae: Implications for Venus Geodynamics

VICKI L. HANSEN AND JAMES J. WILLIS

Department of Geological Sciences, Southern Methodist University, Dallas, Texas 75275
E-mail: vicki@mail.smu.edu

Understanding the nature and timing of tessera formation is fundamental to Venus tectonic and geodynamic models. Tesserae are commonly considered to exhibit complex deformation histories, to represent the oldest global stratigraphic unit, to have formed during a global phase of tesserization, and to require weak lithosphere for their formation. Although these characterizations of tesserae are gaining widespread mention in the literature, they are essentially unsupported by an assemblage of data, yet they figure prominently in the way we frame and address questions about Venus tectonics. Thus they are quickly becoming accepted paradigms despite a lack of scientific foundation. Open discussion of these hypotheses or assumptions is crucial because of their implications concerning geodynamic models of the surface evolution and planetary dynamics of Venus. We examined tessera terrain in Ishtar Terra, crustal plateaus, and as inliers within the plains using high-resolution *Magellan* radar imagery. We describe several types of tessera terrain that record a wide range of structural histories. Fold and S-C terrains are found only in Ishtar Terra; ribbon, lava flow, and basin-and-dome terrains reside within the interior of crustal plateaus, whereas folded ribbon terrain and extended folded terrain comprise margins of crustal plateaus. Inliers are divisible into fracture-dominated and graben-dominated tesserae, although some inliers host early contractional fabrics. The range of deformation histories recorded by the various tessera types indicates that tesserae should not be considered a single map unit. Tessera deformation records local to regional surface strain patterns, and reflects near-surface rheology at the time of deformation. Progressive deformation fabrics in some tessera terrain record changes in shallow crustal rheology through time. Thus structural analysis of individual tessera types and tessera provinces will allow us to better understand the tectonic processes responsible for tessera formation. Tesserae likely formed in several tectonic environments, including (1) as a result of subsurface flow in Ishtar Terra, (2) as sequences of surface-layer extension and contraction in crustal plateaus, (3) as flooded crustal plateaus, and (4) as densely fractured surface layers—fractured as a result of corona and chasma formation. © 1996 Academic Press, Inc.

1. INTRODUCTION

Tessera terrain, known originally as parquet terrain, on Venus is characterized by at least two intersecting sets of structural elements, high relief compared to the surrounding volcanic plains, and unusually high surface roughness at cm to m scale (Barsukov *et al.* 1985, 1986; Basilevsky *et al.* 1986; Sukhanov 1986, 1987; Bindschadler *et al.* 1990). Tesserae constitute about 8–10% of the venusian surface (e.g., Ivanov and Basilevsky 1993, Price and Suppe 1994), and occur as a dominant tectonic terrain of some venusian highlands (crustal plateaus and Ishtar Terra) and as small islands, or inliers, primarily within the plains (Fig. 1). Additional tesserae are almost undoubtedly present but are covered by volcanic plains (e.g., Sukhanov 1986). Understanding the timing and nature of tessera formation is fundamental to our overall knowledge of Venus locally, regionally, and globally.

When and how tesserae formed are challenging pieces to Venus' history puzzle. Prior to *Magellan* (and even post-*Magellan*) many authors considered that tesserae record complex deformation histories (e.g., Barsukov *et al.* 1985, 1986; Bindschadler and Head 1991; Solomon *et al.* 1991, 1992; Bindschadler *et al.* 1992a, 1992b), and that tesserae represent some of the oldest preserved crust on Venus (e.g., Bindschadler and Head 1989, Kaula *et al.* 1992, Senske *et al.* 1992, Squyres *et al.* 1992, Ivanov and Basilevsky 1993, Basilevsky and Head 1995). The interpretation that tesserae comprise the oldest crust on Venus has led to the implication that tesserae are of similar age globally, and can therefore be used as a global time-stratigraphic marker, and, further, formed during a global phase of tesserization (e.g., Solomon 1993a, 1993b; Grimm 1994; Ivanov and Head 1995; Tanaka *et al.* 1995; Basilevsky and Head 1995). Tesserae as a global stratigraphic unit might appeal to geologic mappers, because if this hypothesis is true, regional correlation becomes less challenging. In addition, accepting that Venus underwent an early period of
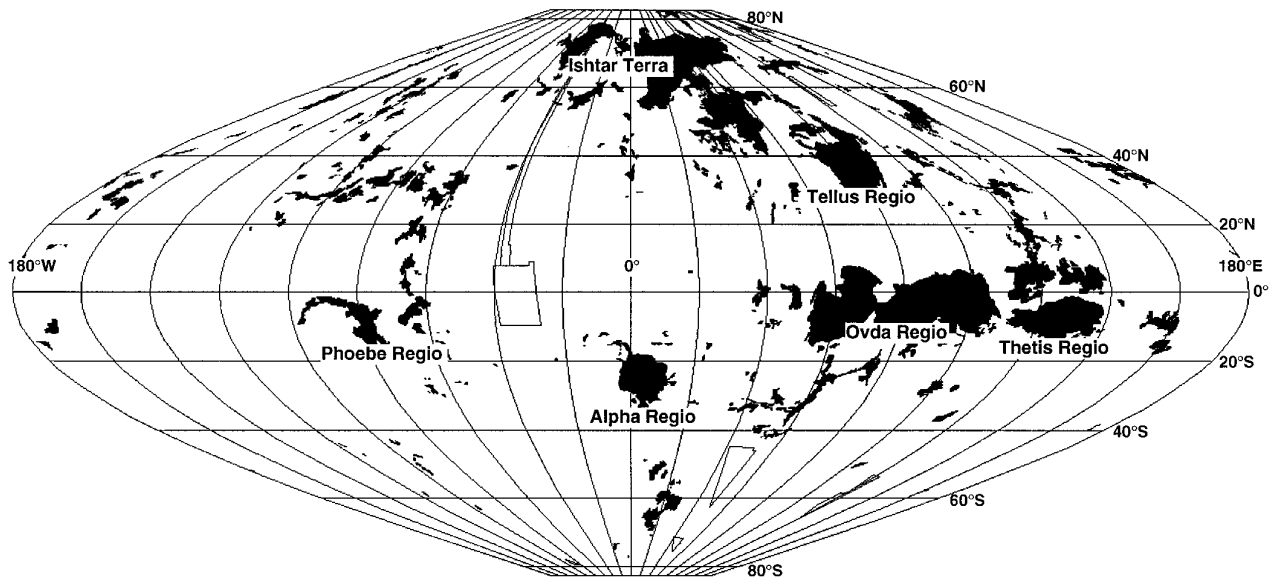
FIG. 1. Sinusoidal index map of Venus tesserae (black) (courtesy of M. Price).

global tesserization might appeal to dynamic modelers, because it begins to delineate stages of venusian evolution; a stage of tesserization might be taken as a time of globally weak lithosphere and can be dynamically modeled (e.g., Solomon 1993a, 1993b; Grimm 1994). As appealing as global synchroneity of tessera formation might be to planetary geologists and geophysicists, we must be able to prove, or at least robustly support, global synchroneity of tessera formation, not assume it.

The conclusion that tesserae record complex deformation (e.g., Barsukov *et al.* 1985, 1986; Bindschadler and Head 1991; Solomon *et al.* 1991, 1992; Bindschadler *et al.* 1992a, 1992b) likely stems, in part, from the fact that tesserae (or parquet terrain) were first described in Soviet *Venera* images, images with resolution near the scale of tessera deformation fabrics. ''Tesserae'' has become a grab-bag term used for *apparently* complexly deformed crust. Interpretations of complexity depend on data resolution; image resolution at a scale below or similar to that of the fabrics may result in an apparent increase in fabric complexity. Deformation fabrics also appear complex if one does not understand how they formed. *Magellan* SAR (Synthetic-Aperture Radar) resolution allows, in many cases, for the delineation of individual linears and for differentiation between folds, fractures, and graben with relatively high confidence; in some cases temporal relations between families of structures can also be interpreted, particularly with computer enhancement of digital images.

We investigated a variety of tesserae (but by no means all) within Ishtar Terra, crustal plateaus, and plains inliers or islands (Fig. 1). A wide range of possible structural histories represented by tessera terrains cautions against uncritical acceptance of the hypothesis that tesserae represent a globally synchronous unit. In fact, our analysis indicates that it is not geologically prudent to consider tesserae as an individual map unit. In the following sections we describe several general styles of tessera terrain, interpret their strain histories, and provide possible models for their formation. We discuss the implications of these results for tessera deformation and Venus evolution, and for geologic mapping and geodynamic modeling.

2. CONCEPTS OF THE STRAIN ELLIPSE

Strain theory, which compares the size and shape of deformed and undeformed materials, is useful for describing structural geometries and kinematics (Ramsay and Huber 1983, 1987; Price and Cosgrove 1990). Strain is described using longitudinal strain, change in line length, and shear strain, related to the angular change of two initially perpendicular lines. Strain is homogeneous if straight and parallel lines remain straight and parallel after deformation, otherwise strain is inhomogeneous. The strain ellipse represents homogeneous strain, and is constructed from the principal strain axes, lines with only longitudinal strain (Fig. 2a). Contractional, extensional, and strike-slip structures can form synchronously, and their orientation is related to the principal strain axes (Fig. 2b). During progressive deformation, the principal strain axes maintain constant orientation (coaxial strain) or rotate (non-coaxial strain). The orientation of structural features may change during non-coaxial strain.

It is possible for a relatively simple strain path to result in a seemingly complex pattern of structures. The geometry
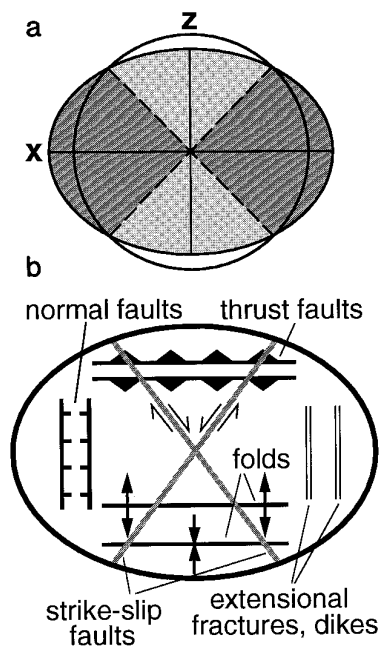
FIG. 2. (a) Finite strain ellipse illustrating regions of finite shortening (light gray) and finite elongation (dark gray), separated by lines of no finite elongation (dashed lines). Principal strain axes are shown by solid lines; X, maximum; Z, minimum. (b) Family of structures that can form synchronously or within the same strain regime.

and kinematics of structures are predictable within strain ellipse concepts, and therefore orientation can be used to constrain temporal relations between structural trends. Documentation of the overall strain patterns and local strain paths within a region is a necessary step in understanding deformation processes.

3. RADAR IMAGE INTERPRETATION

The NASA *Magellan* mission yielded high-resolution (~100 to 250-m resolution) radar imagery of ~98% of the planet. This vast data set hosts an incredible wealth of information for interpreting the structural evolution of the surface of Venus. *Magellan* SAR images derive from echoes of electromagnetic energy pulses transmitted perpendicular to the line of flight of the spacecraft. Analysis of the intensity, time delay, and frequency shift of the echoes produces images in which brightness corresponds to echo strength (Ford *et al.* 1989). Radar brightness is controlled primarily by surface slope and surface roughness. Surfaces oriented approximately perpendicular to the incident beam reflect the greatest radar energy back to the receiver, producing radar-bright areas. Surface slopes oriented away from the radar inhibit reflections, and thus appear darker. Therefore brightness varies with topography and radar beam look angle (Ford *et al.* 1989, Farr 1993). Given uniform slope, smooth surfaces reflect

most of the radar energy away from the receiver and therefore appear dark, whereas rough surfaces (e.g., deformed areas) scatter radar echoes in all directions, resulting in radar-bright areas (Ford *et al.* 1989, Farr 1993).

Surface radar-brightness is therefore a useful tool for structural mapping. Changes in radar-brightness, and the texture of radar-bright areas, allow interpretation of surface orientation and/or surface roughness. Physiographic and geologic features, generally manifested as linears, may be discerned on the basis of shape (straightness or sinuosity), spacing, length, nature of changes between radar-bright and -dark areas (either gradual or abrupt), and whether structures are paired or single (Stofan *et al.* 1993).

Single linears have several forms. Some are long, slightly anastomotic, radar-bright along one side, and have gradual transitions in brightness across them. These features are generally interpreted to be physiographic ridges, with bright radar-facing slopes becoming progressively more radar-dark where they dip away from the radar (e.g., Ford *et al.* 1989, 1993). This effect is enhanced if the ridges are oriented perpendicular to the radar beam, and it weakens with smaller angles to the radar. Ridges are commonly interpreted as folds (e.g., Campbell *et al.* 1983, Solomon *et al.* 1991, Kaula *et al.* 1992, Stofan *et al.* 1993), and thus of contractional origin. Radar-dark areas between bright ridge crests are topographically lower (i.e., valleys), as indicated locally by apparent filling by radar-smooth material, interpreted as flood-type lava flows. Stofan *et al.* (1993) interpreted the gradual tonal transition across ridges as paired light and dark linears, whereas Keep and Hansen (1994) defined them as singular bright linears with gradual tonal changes; either designation is correct.

Other single linears are thin, sharp, and straight, and they show uniform radar-reflectivity and have sharp tonal contrasts to surrounding areas. These sharp linears commonly end against other linears, or other linears end against them, resulting in juxtaposition of contrasting radar-bright areas. On Earth, such features are interpreted as fractures, and we follow this for Venus (e.g., Ford *et al.* 1989, Stofan *et al.* 1993).

Paired linears are commonly straight and parallel. One slope of the pair is radar-bright toward the center, whereas the other is radar-dark, indicating opposite-dipping slopes toward the topographic low center of the linear pair. These features are typically interpreted to be graben, cited as evidence of local crustal extension (e.g., Basilevsky *et al.* 1986, Bindschadler and Head 1991, Solomon *et al.* 1991, Smrekar and Solomon 1992). Graben floors may preserve preexisting radar-brightness contrasts, may be uniformly radar-dark due to volcanic flooding, and/or host radar-bright smaller-scale accommodation structures. Generally, the transitions across one linear to the interpreted graben floor are sharp, in contrast to the gradual transition in radar-brightness across folds.

The relative timing, depth, and dip of some extension fractures may be inferred from their spacing, and orientation with respect to topography. Terminated fractures are younger than through-going fractures, because a through-going fracture acts as a free surface blocking propagation of younger fractures (e.g., Engelder and Geiser 1980, Pollard and Aydin 1988). It is more difficult to interpret temporal relations between intersecting fractures however. If an older through-going fracture is filled it does not act as a free surface, so younger fractures may propagate across it. Also, if a young fracture initiates at greater depth than an old fracture, it may propagate beneath and around the older fracture. In special situations two intersecting sets may form synchronously. Fracture spacing is related, in part, to the depth of a fracture set; closely spaced or penetrative fractures generally indicate shallow depth, and more broadly spaced fractures indicate greater depths (e.g., Engelder and Geiser 1980, Pollard and Aydin 1988). The relative dip of structures may be inferred from their interaction with topography. Steeply dipping structures cut across topography with linear traces, whereas traces of shallow dipping structures follow topography.

For *Magellan* data, some of the above relationships are further complicated. With side-looking radar there is an ambiguity in range introduced by elevation changes (Ford *et al.* 1989). For example, a vertical fracture with a straight strike will appear to wander laterally over varying topography. In addition, layover, or extreme foreshortening, occurs at low incidence angles where topographic peaks are closer than the topographic base to the spacecraft; as a result peaks may appear to ''layover'' adjacent valleys on the radar images (Ford *et al.* 1989, Farr 1993). Layover effects are enhanced by small incidence angles and steep slopes. One of the main effects of layover in terms of structural analysis is that ridge asymmetry, and hence fold symmetry, cannot be uniquely determined from single look-direction data (Farr 1993, Stofan *et al.* 1993), although ridge crest spacing can be used to infer wavelength (Keep and Hansen 1994).

The spatial distribution of structures is also important in determining strain history. During a single deformation episode, different crustal strains may be recorded at different locations. Thus it is important to identify families of linears, interpret their structural nature, infer timing and depth relations between them, and use their spatial distribution to interpret strain history. Where available, we used both right- and left-looking images, and analyzed images both in hard copy and as computer (CD-ROM) images, which allow for digital manipulation and enhancement.

4. TYPES OF TESSERA TERRAIN

Figure 3 illustrates different types of tesserae and possible deformation histories. We describe each type below.

These tesserae are not meant as a classification scheme; they simply represent a sampling of different tessera terrains.

4.1. Fold Terrain

The structural characteristics of much of Atropos Tessera, western Ishtar Terra, are virtually identical to adjacent Akna Montes, consisting of a well-defined linear fabric comprised of elongate (>100 km) ridges and valleys. Following previous interpretations (e.g., Soloman *et al.* 1991) we interpret the linears as folds based on the gradation in radar brightness across the linears. The ridges are antiforms, the valleys synforms. The folds generally trend north-northeast, although local variations exist. Apparent changes along individual folds are primarily an artifact of radar distortion. Because the elevation of antiformal crests changes longitudinally, higher regions are shifted to the west and lower crestal positions are shifted to the east, resulting in apparent changes in local fold orientation. The apparent asymmetry of Akna folds, and locally of Atropos folds, is probably due to radar distortion and layover effects, rather than reflecting true fold asymmetry and structural vergence. Many antiformal crests are superimposed on adjacent synformal valleys to the west, and in extreme cases they overlie the flank of the neighboring antiform. Minor extension fractures locally cut across ridge crests perpendicular to fold trend (Fig. 3a). Folds of eastern Atropos Tessera parallel those of Akna Montes, and fold spacing (6–20 km) remains largely consistent across hundreds of kilometers normal to the structural trend indicating no obvious strain gradient (Hansen and Phillips 1995). Many of the synformal valleys are flooded by lava derived from unnamed paterae to the north (74°N, 313°E). Some flooded valleys are deformed by wrinkle ridges and fractures in a strain regime consistent with Akna/Atropos deformation, indicating likely synchroneity between patera volcanism and late Akna/Atropos tectonism (Willis and Hansen 1995).

The main difference between Atropos Tessera and Akna Montes is their elevation—Atropos Tessera is topographically lower and thus has more lava-flooded valleys. Akna/Atropos deformation can be explained by simple unidirectional contraction (Fig. 3a). The relatively simple structural history and the lack of obvious strain gradients across Atropos indicate that deformation likely results from stress transmitted from below (e.g., Keep and Hansen 1994, Hansen and Phillips 1995).

4.2. ''Lava Flow'' Terrain

The patterns in some tesserae, including parts of central Ovda Regio (Fig. 3b), exhibit remarkable similarities to pahoehoe lava flows, as originally noted by Sukhanov (1986). At Ovda the dominant structural fabric is made

FIG. 3. Types of tessera terrain and plausible models. Column 1—F-MIDR SAR images (approximately 180 km by 110 km); column 2—illustrative stylized maps of dominant structural forms (except in the "lava flow" pattern example, the sketch maps are generalizations and are not maps of the respective SAR images); column 3—models of formation; column 4—geomorphic locations of tessera types. Symbols correspond to structural forms labeled in Fig. 2b. Strain ellipses show finite bulk strains and include dominant structural elements formed in each strain regime. (a) "Fold terrain," Atropos Tessera and Akna Montes (F-MIDRP.70N310;1). (b) "Lava flow terrain," Ovda Regio (F-MIDRP.05S087;1). (c) "S-C terrain," Itzpapalotl Tessera (F-MIDRP.75N332;1, image rotated counterclockwise ~30°). (d) "Folded ribbon terrain" and "extended fold terrain," Ovda Regio (F- MIDRP.05N098;1). (e) "Basin-and-dome terrain," Alpha Regio (F-MIDRP.25S003;1). (f) "Star terrain," Phoebe Regio (F-MIDRP.05S279;1). (g) "Small inlier," unnamed plains (F-MIDRP.25S292;1;C1-MIDRP.30S297;201).

up of anastomosing and curvilinear ridges with ridge-to-ridge spacing varying from <2 to 15 km, and ridge length up to 90 km. We interpret these structures as folds based on the gradational radar tones across the ridges. Smaller-scale folds are ''superimposed'' on these larger-wavelength structures. The axes of the small folds are locally both parallel to and at an angle to the longer-wavelength folds. Synformal valleys are locally radar-dark, and interpreted as smooth, lava-flooded valleys. This tessera type displays geometries similar to folds preserved on the surface of pahoehoe lava flows. It is on the basis of this comparison that we call this tessera type ''lava flow terrain.''

The cooling crusts of lava flows commonly deform in response to continued movement of more fluid lava beneath (Stokes and Varnes 1955, Green and Short 1971). This deformation may be manifested by folds of variable orientation. As the underlying lava moves, parts of the overlying crust may respond differently, resulting in variations in surface fold orientation. In the case of lava flow tessera terrain, we envision a process similar to the deformation of lava crusts, in which the upper venusian crust is displaced and deformed differentially by movement, uniform or not, of material beneath the deformed surface layer.

4.3. S-C Terrain

Itzpapalotl Tessera, a northwest-trending package of tessera ~800-km long and 250-km wide, forms the northern region of Ishtar Terra. Itzpapalotl is bound to the northeast by the 10°–20° slope of Uorsar Rupes and to the southwest by Freyja Montes. A structural fabric comprising of two principal families of structures dominates western Itzpapalotl (Hansen 1992) (Fig. 3c). A penetrative fabric of tightly spaced (<1 km) ridges trends north-northwest. The gradational change in brightness across the crest of these structures indicates that they are folds. Through-going, west-northwest-trending, spaced (15 to 50 km) linears, which form lava-flooded lows, appear, at first glance, to cross-cut the tightly spaced folds. However, the tightly spaced folds curve into parallelism with the spaced through-going linear valleys, and locally the spaced linears curve into parallelism with the tightly spaced fold fabric, indicating that the fabrics are broadly contemporaneous. The spatial development of these two families of structures defines a regionally consistent asymmetric fabric geometry that characterizes Itzpapalotl. A third set of structures, locally developed paired fractures, completes the structural fabric. These paired fractures, 5- to 20-km long and ~2-km wide, strike perpendicular to the penetrative folds. The sharp change in brightness across these linears indicates that they are likely small graben.

The penetrative folds, through-going linears, and the small graben can all be related within a simple non-coaxial

bulk strain regime (Hansen 1992); therefore it is not necessary to call on different deformation events to form this group of structures. In fact, mutual cross-cutting relations between the penetrative folds and the spaced linears do not support a polyphase structural history. Deformation at Itzpapalotl is geometrically akin to S-C tectonic fabrics (see Berthé *et al.* 1979, Simpson and Schmid 1983, Lister and Snoke 1984), in which non-coaxially deformed material initially develops a penetrative schistosity, S, at an angle to the shear zone; with continued displacement, strain is partitioned into shear planes, C (from *cisaillement*, French for shear), parallel to the shear zone boundary. Deformation of S is dominantly coaxial shortening and extension, illustrated at Itzpapalotl by contractional fold ridges with superimposed perpendicular graben. Deformation along C surfaces is dominated by shear strain, left-lateral at Itzpapalotl. Although the result appears complex, the deformation is simply progressive non-coaxial strain. Thus, Itzpapalotl Tessera (Fig. 3c) represents an example (perhaps uniquely) of tessera formed by distributed crustal-scale non-coaxial shear.

Itzpapalotl Tessera is much broader than regions of non-coaxial strain on Earth; however, Grimm and Solomon (1988) predicted that large-scale motion on Venus should be reflected in distributed deformation, rather than narrowly focused as failure along plate boundaries. Therefore the scale and geometry of shallow crustal-level venusian structures may be more closely correlative with deeper crustal levels of terrestrial structures which broaden and are more widely distributed at depth (e.g., Sibson 1984). Crustal-scale shear fabrics, comparable in scale and geometry to Itzpapalotl fabrics, have been described for upper greenschist facies to amphibolite facies Proterozoic rocks in northeast Brazil (Cornsini *et al.* 1991).

With regard to tessera formation, Itzpapalotl represents a region that records a simple, rather than complex, deformation history, despite complex-appearing deformation fabrics. It also demonstrates that strike-slip translation of the venusian surface is possible, if not common.

4.4.a. Extended Fold Terrain

Numerous superimposed large-scale paired linears that trend nearly perpendicular (>70°) to the regional ridge orientation characterize many tessera terrains, including parts of Alpha, Ovda (Fig. 3d), Thetis, and Tellus regiones, and Ananke and Laima tesserae. Northwest-trending ridges with 3- to 15-km spacing extend for hundreds of kilometers along the northeastern boundary of Ovda Regio (Fig. 3d). The gradational tonal changes across the axes of the ridges reveal the folded character of these structures (as noted by many workers). The folds occur over an area 250 km in width (perpendicular to fold trend) with no obvious change in fold spacing, likely reflecting a lack of

strain gradient. The folds are cut by northeast-trending paired linears marked by sharp changes in radar brightness, interpreted as graben, or graben systems. Individual graben range up to 10-km wide, with graben systems locally as wide as 35 km. The graben, lens-shaped in plan view, pinch out along their strike, or feather into a number of narrower graben. Graben systems range up to ~100-km long. A smaller, less well-developed, but regionally continuous, structural fabric parallel to the graben occurs in northeastern Ovda. This fabric, which we call "ribbon terrain," is discussed in Section 4.4.b. The graben are relatively radar-bright indicating rough sides and floors.

Most workers agree that these folds and large graben record an early phase of contraction followed coaxially by extension (e.g., Bindschadler and Head 1991; Solomon *et al.* 1991, 1992; Bindschadler *et al.* 1992a, 1992b; Basilevsky and Head 1995). This sequence of deformation could occur by a change from contraction to extension due to either (1) progressive deformation, or (2) two separate unrelated events. Detailed documentation of temporal relations is necessary to distinguish between these two cases. In both cases, however, the strain histories are not complex because there is no change in the orientation of the principal strain axes.

4.4.b. Folded Ribbon Terrain

The fold terrain in northeastern Ovda hosts another fabric common to tessera terrain. The fabric, herein called ribbon terrain (Figs. 3 and 4), is comprised of sharp, parallel, radar-dark and radar-bright paired linears, oriented perpendicular to fold axes. Topographic lows, ~2- to 7-km wide, between paired linears, can be traced over 50–100 km across antiformal ridges and synformal valleys without apparent change in width or depth of the intervening low. We interpret the linears as steep faults (breaks) based on examination of similar structures in Fortuna Tessera (Fig. 4, discussed below). The linears appear warped or bent across the fold crests in the direction of the spacecraft, a likely result of foreshortening rather than a real change in orientation. Ribbon terrain differs from the previously described graben (Section 4.4.a.) in that ribbons are longer, more closely spaced, and extremely consistent along strike. The ribbons parallel the graben although the character of the two structures is quite different. Graben display lenticular shape in plan view with rough sides and floors, whereas ribbons have much longer aspect ratios (hence their name) and their floors are radar-dark—therefore, smooth.

The character of ribbon terrain is more easily defined using an example from southern Fortuna Tessera (Fig. 4a). North-trending ribbons dominate the tectonic fabric at this location. Individual ribbons are ~2- to 7-km wide and ~30- to 150-km long, and pinch out along strike; in concert

ribbons describe a coherent linear pattern with consistent trend over hundreds of kilometers. To the south, gentle west-northwest-trending folds are evident as the ribbons describe parallel, but slightly sinuous, paths. Across the antiformal crests ribbons consistently appear bowed or bent to the west (toward the spacecraft during imaging), likely the result of layover.

The overall three-dimensional character of ribbon terrain can be inferred from the interaction of the ribbons with lava-flooded synformal valleys. A west-trending synformal valley transects the ribbon terrain in the northern portion of Fig. 4a. Assuming low lava viscosity, consistent with the radar-dark (and hence smooth) character of the valley fill, the lava would have defined a horizontal plane during flooding, which we assume remains essentially horizontal at present. The "shoreline" of the valley fill would also be horizontal, thus radar foreshortening does not affect the shoreline position, unless adjacent areas with topographic relief overlay the shoreline. The geometric configuration of trough embayments is such that the western shoreline of the individual trough embayments is unmodified by radar effects, but west-facing slopes defining eastern margins of troughs overlay part of the flooded valley, locally obscuring the real shoreline. Therefore, the shoreline records strike of the fold limbs, and the strike of the ribbon ridges, troughs, and bounding structures of the ribbons—thus the shoreline relates to the ribbon's cross-sectional character (Fig. 4b). The bottoms of the troughs are straight strikes parallel to the fold limbs. The folds are generally non-plunging, based on the parallelism between trend of fold crests, and fold-limb strike.

The embayment angle, β, reflects the angle between fold-limb strike and the strike of the ribbon-bounding structures; the relation of β to three-dimensional ribbon geometry depends upon whether ribbons postdate or predate folds. If the ribbons *postdate* the folds, β is independent of the dip of the ribbon-bounding structures, and reflects the strike change between fold limb and bounding structure. If the ribbons are perpendicular to the fold crests, as in Fig. 4, then β should be 90°. The bounding structures result in predictable patterns as they cross the fold crest—vertical structures should cross-cut the folds with no structural deflection, whereas dipping structures should exhibit a bowed appearance with the graben widening as elevation increases (e.g., Baldwin 1971, McGill 1971, Golombek 1979). Ribbons at Fortuna Tessera maintain consistent width along trend, with no widening of troughs at fold crests; opposite-facing slopes exhibit similar curvature, a probable artifact of radar foreshortening, thus consistent with steeply dipping ribbon-bounding structures. If the ribbons *predate* the folds, the strike of the shoreline segment of the bounding structures records their present strike, as modified from their original strike due to folding. In this case, β records an apparent dip of the ribbon-
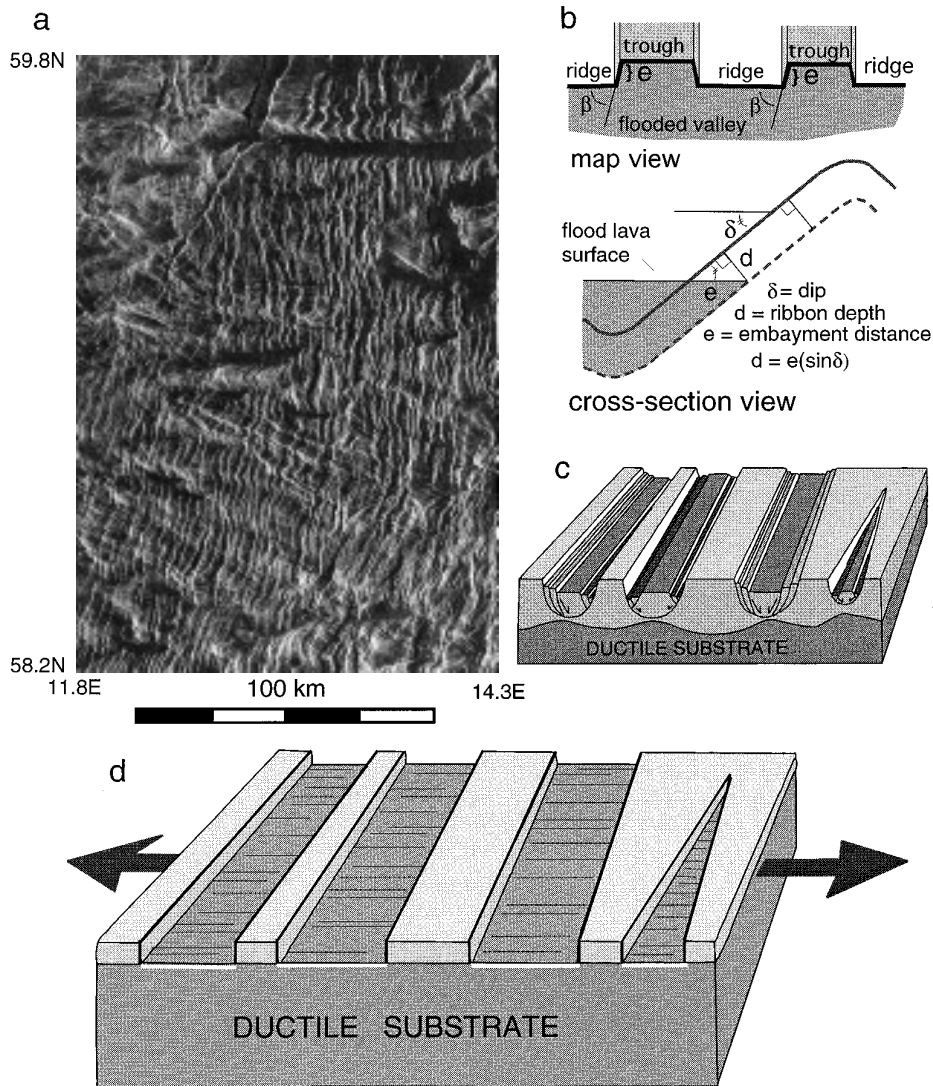
FIG. 4. Ribbon terrain in southwestern Fortuna Tessera. (a) Ribbon terrain in a southwestern portion of SAR F-MIDR.60N016;1. (b) Map view and cross-sectional diagrams defining embayment angle, β, and embayment distance, e, and illustrating how e and fold limb dip, δ, relate to ribbon depth, d. (c) Block diagram of a graben model for ribbon formation; note that the "floors" of the troughs are not flat or smooth, and that in order to accommodate space problems the troughs host many faults parallel to the graben-bounding faults and a ductile substrate is required. (d) Open fracture model of ribbon terrain formation. The surface layer (light gray) deforms in a brittle fashion while the substrate deforms in a ductile fashion. Maximum extension is perpendicular to the trend of the resulting ribbon troughs. Lineations within the troughs describe the direction of stretching. White lines within troughs mark the area of the troughs which expand with progressive extension.

bounding structures. β describes an angle of $>75°$ conservatively, and could be 90° (essentially at the limit of data resolution); therefore the true paleodip is at least $>75°$ (apparent dip $\leq$ true dip). Therefore the dip of the ribbon-bounding structures must be 75°–90°. Both hypotheses of ribbon-fold temporal relations favor a relatively steep dip angle (75–90°) for ribbon-bounding structures. The parallelism of the ribbons and the lack of widening of graben across the fold crests are most consistent with early ribbon formation and with steep ribbon-bounding structures modified slightly by rotation along fold limbs.

The distance that lava embays the subsidiary ribbon valleys is a function of ribbon depth and fold-limb dip (Fig. 4b), but it is independent of the dip of ribbon-bounding structures. The ribbons must be significantly shallower than the amplitude of the folds because the main valley lava does not fill the ribbon valleys toward antiformal crests. Main valley fill embays the ribbon valleys a maximum of 2.25 km, and generally <1.5 km; using these distances, and an assumed 30° dip of the antiformal limbs, results in ribbon depths of ≤1.13 and <0.75 km, respectively. Thus ribbon troughs may be as deep as 1.13 km, but are generally <0.75-

km deep. The similar character of flooding in each adjacent ribbon valley indicates that ribbon depth is the same for adjacent ribbons and is consistent along strike, given that the main valley intersects a host of ribbons that pinch out along strike.

Any model for ribbon formation must account for the regular, closely spaced, long linear, shallow ($\sim \leq 1$ km), flat-bottomed, and steep-sided troughs. Dips of $75°–90°$ for the trough sides are not consistent with classic fault theory (e.g., Anderson 1951), which predicts normal faults of $\sim 60°$, although steeper fault angles may result under near-surface transitional-tensile failure conditions or due to pre-existing weaknesses (e.g., McGill 1979, Price and Cosgrove 1990). However, the regular spacing, long linear character, consistent shallow trough depths, and flat-floored troughs—within individual ribbons and across the population of ribbons—are not easily accommodated by normal fault-graben structures (Fig. 4c). Horst and graben structures would not be expected to have graben of equal depth, of such regular close spacing with the width of the horst equal to the width of graben, with aspect ratios of $>10:1$, and with absolute regularity of alternating horst and graben. In addition, space problems inherent to block down-dropping require synthetic and antithetic accommodation faults (e.g., Price and Cosgrove 1990, Twiss and Moores 1992). However, ribbon trough bottoms are radar smooth and exhibit no internal relief. Accommodation structures should be observable in SAR images, unless the graben valleys were filled after graben formation. The radar bright interior of the graben described in Section 4.4.a may reflect internal accommodation structures; however, ribbons do not. If the flat, smooth bottoms of the ribbon troughs result from post-graben flooding, ribbon formation and flooding must predate folding. The graben model also requires a ductile substrate within the crust at or below the level at which the graben structures shallow (Fig. 4c) (e.g., McGill 1979, Price and Cosgrove 1990, Twiss and Moores 1992).

Alternatively, ribbon terrain formation could consist of steep bounding faults that cut through an upper brittle layer down to a ductile layer, and thus maintain constant depth in adjacent ribbon troughs (Fig. 4d). In this model, extension results in tensile fracturing of a thin (≤ 2 km) brittle surface layer above a ductile substrate. The troughs represent open fractures, and would be flat-bottomed and smooth. The width of the ridges between adjacent ribbon troughs may relate to brittle layer thickness and strength. The depth of the resulting ribbon troughs is equal to the thickness of the brittle surface layer. Stretching a chocolate-covered caramel candy bar provides an analog. Assuming a homogeneous isotropic brittle layer, maximum elongation is perpendicular to the trace of the ribbons, and is recorded by trough widths, although ribbon-bounding structures could also represent faulting along preexisting fractures. Elongation of the brittle surface layer might be

as high as 50–100%. We favor the open fracture model because it better explains (1) the high aspect ratio and consistent narrow spacing of the ribbons, (2) the consistent depth of individual and adjacent troughs, and (3) the flat-bottomed, smooth floors of the troughs.

Fold formation likely postdates ribbon formation, although locally the two may form synchronously. The observed geometric relations at embayed troughs favor a pre-fold origin of ribbons. Pervasive formation of narrow ribbons across large areas, with extremely long aspect ratios and consistent width of individual ribbons, is most easily explained in a flat homogeneous layer—stress, and thus strain heterogeneities due to preexisting folds, would almost certainly preclude the formation of parallel ribbon structure over large areas. The open fracture and graben models for ribbon formation require a rheological contrast in the upper crustal layers. Such a contrast also is most easily envisioned in a flat—not yet folded—layer, although one might argue that special (i.e., highly constrained) circumstances could result in rheological layering parallel to the fold structure, rather than parallel to a horizontal surface.

Regardless of model of formation of ribbon terrain, whether by graben or open fracture mechanisms, three key points arise: (1) ribbons record extension, (2) a ductile substrate is required at relatively shallow crustal levels, and (3) ribbons predate folds. The major difference between these two models is the depth to the ductile substrate, being a bit deeper in the graben model, and the amount of overall extension recorded, with greater total extension accommodated by the open fracture model.

Ribbon terrain may be affected by younger folds or graben. In parts of Ovda and Fortuna, fold and ribbon orientations are compatible within the same overall strain regime (that is, there is no evidence for a rotation of the principal strain axes, therefore strain is coaxial). Thus, it is plausible that extension normal to the resultant ribbons evolved progressively into contraction parallel to the ribbon troughs without major rotation of the principal strain axes. Parts of Ovda apparently experienced renewed extension following folding (Fig. 3d); post-fold extension resulted in the formation of large graben that cut earlier-formed ribbons and folds. Late graben formation could have been coaxial with both ribbon and fold formation. Many regions of folded ribbon terrain apparently did not experience younger, or continued extension because these regions do not show large graben that clearly cross-cut antiformal ridges.

The graben described in Section 4.4.a are generally wider, shorter, and deeper than the ribbon structures, and their radar-bright interiors likely reflect accommodation structures required by graben formation. In addition, their spacing is less consistent than that of ribbon structures. The large graben cut both the brittle and the ductile layers

required by the ribbon fabric. Therefore the graben formed later than the ribbons, and the rheological structure at the time of graben formation was different than the rheological structure at the time of ribbon formation. The change in rheology might reflect thermal decay (cooling), resulting in downward migration of the brittle/ductile front with time, consistent with late formation of the graben relative to folding.

Some tesserae display two or more ribbon suites. These may represent (1) fracturing along preexisting weaknesses, (2) synchronously formed conjugate ribbons with maximum elongation perpendicular to the acute bisectrix, or (3) successive local extension events with changes in orientation of the principal strain axes. In some locations, fractures that parallel the ribbons and cross-cut lava-flooded synformal valleys may represent reactivated ribbon structures.

In summary, ribbon formation records crustal extension of a relatively large flat region, and requires specific rheological structure of near-surface layers of the crust during the time of formation. Therefore the occurrence of ribbon terrain places stringent rheological constraints on the early stage of extension in tessera terrains that host ribbon terrain.

4.5. Basin-and-Dome Terrain

Many tesserae consist of arcuate ridges and troughs, including parts of Alpha Regio (Fig. 3e), and perhaps represent the most complex appearing of tessera types (e.g., Bindschadler and Head 1991; Solomon *et al.* 1991, 1992; Bindschadler *et al.* 1992a; Phillips and Hansen 1994). Generally, this style of tesserae occurs within the center of crustal plateaus. The largest-wavelength structural fabric is comprised of ridges spaced 15–25 km. A dominant structural trend is generally present, although individual ridges exhibit substantial variability in orientation; many ridges are curvilinear, possibly representing two or more intersecting populations, resulting in an egg-carton, basin-and-dome pattern. Previous workers interpreted that basin-and-dome fabrics record polyphase folding, whereby the variation in ridge trend represents resultant fold interference from superposed folding events (Bindschadler *et al.* 1992a, Solomon *et al.* 1992, Phillips and Hansen 1994). We agree that many basin-and-dome fabrics record dominant contraction. However, we also recognize that extensional structures dominate some basin-and-dome terrains, whereby the ridges are not contractional folds, but rather structural and topographic highs bordered by large-scale trough-forming graben with internal small-scale accommodation faults. Additional basin-and-dome terrains host both folds and graben.

Some areas also exhibit pervasive early-stage extensional ribbons, commonly oriented at high-angle to ridge crests. The example from Alpha Regio illustrates regional northwest-trending ribbons, northeast-trending folds, and minor extension fractures (Fig. 3e). Ribbons can be traced across basin-and-dome patterns, and predate formation of these longer-wavelength structures.

The change in the orientation of the strain regimes recorded by basin-and-dome structures cannot be explained by progressive non-coaxial strain; rather these structures require true polyphase deformation.

4.6. "Star" Terrain

Classic tesserae at central Phoebe Regio (Fig. 3f) is comprised dominantly of fractures and extensional graben. At Phoebe, linears trend in many directions, locally describing a radiating or "star" pattern. We interpret the linears as fractures and/or graben based on the sharp tonal contrast across them. Attempts to decipher individual temporal relations between dominant structural trends (e.g., north-northwest-trending versus east-trending) or between fracture patterns (e.g., radial or orthogonal) have not proved successful. Such temporal relations would, in fact, be very difficult to constrain given that individual structures could penetrate to variable depths, or be variably filled after their formation resulting in ambiguous cross-cutting relations. Despite this ambiguity, there appears to be a correlation between the density and width of graben, and local elevation within central Phoebe Regio (Fig. 5). Regions that lie above 1 km above mean planetary radius (MPR) appear to host more graben and wider graben than those regions below 1 km above MPR; similarly regions above ~1.5 km above MPR appear to host yet more graben, and yet wider graben. Although the apparent widening of graben with elevation might be a geometric artifact (e.g., Baldwin 1971, McGill 1971, Golombek 1979), and might therefore not reflect an increase in strain with elevation, the correlation of graben density and elevation indicates a correlation between strain and elevation. The star pattern of graben appears most prominent at elevations above 1.5 km above MPR.

We postulate that dilation of the crust due to uplift resulted in previously formed fractures opening into well-defined graben with no apparent consistency of timing relations between individual graben (similar to scored bread dough during baking), as well as in the formation of new fracture sets. The degree to which each fracture set opens depends on fracture depth and fracture orientation relative to the uplift pattern. The more a region has been uplifted, the greater the dilation, and the greater the density and width of graben. Radiating (star) patterns of graben may represent areas of localized uplift within the regional warping (Figs. 3f and 5).

Following this model, the point at which a terrain is considered tesserae, before or after doming, is debatable.

FIG. 5. SAR image of central Phoebe Regio (F-MIDRP.05S279;1). Contours represent altimetry in km above mean planetary radius. Degree of graben development and fracture/graben density are correlative with elevation—high elevations exhibit wider graben and increased number of graben, whereas low elevations are fractured (minor graben development) or covered by volcanic plains. Local hachures indicate down-slope direction.

By definition, intersecting sets of structures constitute tessera terrain, and sets of fractures at central Phoebe Regio prior to doming could be considered tesserae. (However, numerous areas of Venus' crust with intersecting fracture sets are not classified as tesserae.) On the other hand, if arching and resultant widening of preexisting fractures into graben mark the time of tesserization, then tessera formation might coincide with the most recent doming of a region. In the case of central Phoebe, local uplift or warping of the surface is probably relatively young, based on the correlation of graben development with present elevation. Tesserae in parts of Phoebe Regio thus may provide an example in which a seemingly complex structural pattern of intersecting graben can be explained by broad doming of previously fractured crust, rather than calling upon multiple extensional events.

4.7. Tessera Inliers

Reconnaissance survey of 113 hard-copy F-MIDR images with tessera inliers reveals that inliers are dominated by extensional deformation fabrics. Fractures and graben dominate the tectonic fabric of inliers in 80% of the

F-MIDRs, folds dominate inliers in 5%, and 15% display inliers that host both contractional and extensional structures (percentage by number, not area, of inliers). Where contractional and extensional structures are present, folds may predate or postdate extensional structures. Extension-dominated inliers are broadly divisible into fracture-dominated (Fig. 3g) and graben-dominated tesserae. Fracture-dominated inliers are small, relative to graben-dominated inliers, which comprise the large inliers. Fracture-dominated inliers, marked by narrow fractures of two or more orientations, typically lack folds and lens-shaped graben. Adjacent inliers commonly lack continuity in fracture orientation from one inlier to the next. Graben-dominated inliers are radar-bright making structural analysis difficult in many cases. In some cases graben-dominated inliers host early contractional fabrics, such as large inliers with arcuate boundaries—some large inliers are themselves large arcs. The arcs typically host folds parallel to their trend, which are cut by graben. Large inliers also locally host basin-and-dome terrain, and early-formed ribbon terrain is present locally.

An elongate 200 × 400-km tessera inlier (~27°S, 294°E), a plains tessera patch surrounded by flood-type lava flows,

illustrates a number of features typical of tessera inliers (Fig. 3g). The boundary of the inlier with the flooded plains is sinuous, describing an irregular shape of tesserae, and indicating very little total relief of the tessera interior. The boundary with the surrounding plains is locally sharp or diffuse. The tessera structural fabric is made up of two or more intersecting families of linears. In this case penetratively developed, tightly spaced fractures and graben trend northwest, and fractures and graben trend northeast to north-northeast. In addition, locally developed, very penetrative (tightly spaced) northeast-trending linears that are either fractures or folds parallel the northeast-trending graben. The shallow angle of these features relative to the radar beam direction, together with their spacing at or below the resolution of the F-MIDR image, contribute to the lack of clarity of these structures. Two prominent east-northeast-trending graben (<4-km wide) cut the above fabrics, and are flooded by lava. Local northwest-trending linears that traverse these prominent graben may result from structural reactivation. Variable embayment of the tessera terrain by lava flows, and subsequent fracturing of the flood lava, presumably record several iterations of deformation and flooding by lava. South of the part of the inlier shown in Fig. 3g, Peck Crater probably postdates some, or perhaps most, of the tessera deformation, and predates the most recent flooding. Inlier 27S294, and others like it, may have formed by variable and consecutive extensions of the surface layer. The extensions could result from a variety of strains including strain associated with cooling, tectonic strain of corona formation, rift formation, or simply extensional strain of local crustal regions.

4.8. Summary

The types of tessera terrain described herein occur in specific tectonic regimes (Fig. 3). Deformation akin to fold terrain (4.1), the simplest of the types, occurs in Atropos Tessera, the Ishtar mountain belts, and planitia ridge belts. Itzpapalotl Tessera may preserve a unique example of S-C terrain (4.3). Lava flow (4.2) and basin-and-dome (4.5) terrains occur within the interior regions of the crustal plateaus Alpha, Ovda, Thetis, and Tellus; and folded ribbon (4.4.b) and extended fold (4.4.a) terrains occur along the margins of these same crustal plateaus. Ribbon terrain (Fig. 4), which occurs commonly throughout crustal plateaus and large inliers, is conspicuously absent in the Ishtar deformed belts (except Fortuna Tessera) and planitia belts. Star tessera terrain (4.6) is apparently relatively uncommon and occurs dominantly in central Phoebe Regio. Large inliers or large tracts of tesserae, such as Ananke and Laima tesserae in the northern hemisphere, are typically made up of basin-and-dome and extended fold (±ribbon) terrain; lava flow terrain and star terrain may be present locally. Small tessera inliers seem to comprise two general groups: (1) fracture-dominated terrain which likely record small overall strain, and (2) radar-bright graben-dominated terrain, which may record higher overall strain, and which may represent highly extended crustal plateau tesserae (e.g., ribbon terrain, folded ribbon terrain, extended fold terrain, lava flow pattern terrain, and basin-and-dome terrain). Eastern Fortuna Tessera includes tracts of ribbon terrain, folded ribbon terrain, extended folded terrain, basin-and-dome terrain, and possibly lava flow pattern terrain. Western Fortuna shares similar structural aspects with fold terrain, such as Atropos Tessera.

5. DISCUSSION

Tesserae are generally interpreted as geologically old terrains characterized by complex, often polyphase, deformation patterns and histories (e.g., Barsukov et al. 1985, 1986; Bindschadler and Head 1991; Solomon et al. 1991, 1992; Bindschadler et al. 1992a, 1992b). In addition, tesserae are considered to have formed during a global phase of tesserization (e.g., Basilevsky and Head, 1995; Ivanov and Head 1995; Tanaka et al. 1995). The differences in the structural histories of the tessera types (1) demonstrate that tesserae are not necessarily formed by complex geologic histories, (2) illustrate that not all tesserae are formed by similar mechanisms, and (3) bring into question the treatment of tesserae as a single global map unit. If tesserae are not a single map unit, the hypothesis that tesserae formed at the same time, or represent a globally coherent stratigraphic unit is incorrect.

5.1. Are Tessera Terrains Complexly Deformed?

Many authors consider that tesserae record complex deformation histories (e.g., Barsukov et al. 1985, 1986; Bindschadler and Head 1991; Solomon et al. 1991, 1992; Bindschadler et al. 1992a, 1992b). Of the tessera types described, six formed by arguably straightforward geologic histories. Therefore, although some tesserae may exhibit evidence of multiple deformation, in general tesserae do not require complex strain histories. Furthermore, the term "complex ridged terrain (CRT)," used by many synonymously with tesserae, carries invalid connotations. "Complex" implies a complexity of deformation history. "Ridge" defines an elongate topographic crest. Although actually independent of origin, ridge is almost exclusively used interchangeably with fold (e.g., ridge belts, wrinkle ridges), implying a contractional origin, yet not all tessera fabrics record contraction.

5.2. Tesserae as a Global Stratigraphic Unit?

Tesserae are commonly the oldest local unit on Venus (e.g., Bindschadler and Head 1989, Kaula et al. 1992, Senske et al. 1992, Squyres et al. 1992, Ivanov and Basilevsky

1993, Basilevsky and Head 1995). Some workers have extended this observation to imply that tesserae are of similar age globally, and can therefore be used as a global time-stratigraphic marker, and, further, formed during a global phase of tesserization (e.g., Solomon 1993, Grimm 1994, Ivanov and Head 1995, Tanaka *et al.* 1995, Basilevsky and Head 1995). This hypothesis remains to be tested, and it must be critically evaluated due to its major implications for Venus geodynamics. Several independent lines of reasoning caution against acceptance of this hypothesis:

1. Although tesserae are typically the oldest local unit, this is not the case everywhere (e.g., Gilmore and Head 1992, Chapman 1995, Willis and Hansen 1995). (By definition tesserae are actually never the oldest, because a unit must exist prior to deformation.)

2. Even if tesserae were everywhere the oldest local unit, that by no means requires that all tesserae formed at the same time. To use an analogy from Earth, relative dating methods, including the principles of superposition, original horizontality, and cross-cutting relations, indicate that crystalline metamorphic rocks are the oldest rocks at separate localities. Prior to absolute dating techniques most gneisses were mapped as Precambrian, implying a level of global synchroneity. Absolute dates reveal, however, that gneissic rocks range in age from greater than three billion years to near present. A global time-frame is necessary, yet missing, for establishing synchroneity (or diachroneity) of tesserae.

3. The quantification of time on Venus presently relies on the impact crater record (e.g., Phillips *et al.* 1992, Schaber *et al.* 1992, Phillips 1993, Ivanov and Basilevsky 1993, Herrick 1994, Price and Suppe 1994). However, statistical problems associated with the limited number of craters (~950), and interpretation of what the calculated ages mean (e.g., "production age" or "retention age") have contributed to dramatically different interpretations of Venus' surface age and evolution (Phillips and Hansen 1994). Uncertainties in the flux rate of meteoroids (overall rate and temporal changes thereof), atmospheric effects toward crater production, and regression fits on the crater size/frequency distribution result in large variations in age estimates.

In order for there to be a small probability that an anomalous crater density is not due to chance, an individual area must be larger than 10 million km^2, and a region as large as 20 million km^2 could record anomalous crater density due to chance (Phillips *et al.* 1992), yet the largest patches of tesserae are each less than 10 million km^2 (Fig. 6) (Basilevsky and Head 1995). Thus, variations in crater densities of *all* individual tessera patches may be attributable to chance; therefore age comparisons between individual tesserae or with other units are not practical.
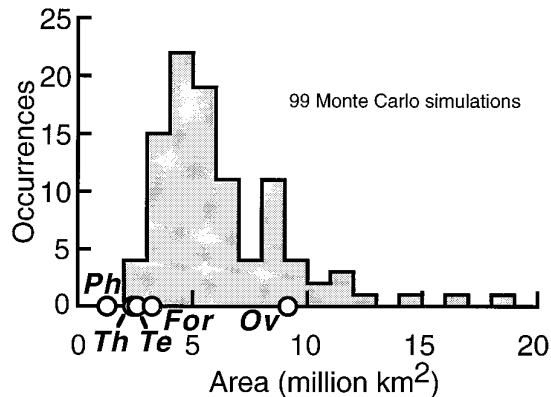
Crater counts from total tesserae carry with them the

FIG. 6. Histogram of the largest patch sizes of anomalous crater density found from 99 Monte Carlo simulations (Phillips *et al.* 1992) with sizes of individual large tessera patches shown: Ph, Phoebe; Th, Thetis; Te, Tellus; For, Fortuna; Ov, Ovda (Basilevsky and Head 1995). In order for there to be a small probability that an anomalous crater density is not due to chance, an individual area must be larger than 10×10^6 km^2, and a region as large as 20×10^6 km^2 could record anomalous crater density due to chance (Phillips *et al.* 1992).

assumption that all tesserae represent a single map unit formed within a very short time relative to the impact history (~10 myr), an assumption challenged by our analysis. Ivanov and Basilevsky (1993) concluded on the basis of large craters (>16 km diameter) that, on average, tesserae are older than non-tessera terrains. Herrick (1994), using all craters, stated that the excess is not statistically significant. Even if tesserae could be shown to be "on average" statistically older than non-tessera terrains, this does not require that *all* tesserae are older than *all* other terrains—only that the *average age of tesserae* is greater than the *average global surface age* (Phillips and Hansen 1994). Average ages may provide useful global estimates, but they do not allow temporal correlation of spatially separate regions.

The importance of a global temporal framework. A global temporal framework is of particular importance to not only tessera formation, but also to planetary geodynamic models. Interpretations of global synchroneity or diachroneity (Fig. 7) both explain existing temporal data, yet require completely different geodynamic models to explain their contrasting histories—global synchroneity favors catastrophic models, whereas global diachroneity favors non-catastrophic models. Evolutionary models may be favored by either end-member, depending on rates of evolutionary changes (e.g., Solomon 1993). Because global synchroneity or diachroneity become starting assumptions upon which geodynamic models are built, and because these assumptions and resulting models are essentially mutually exclusive, interpretations of global temporal relations must be robustly tested and verified. Time is such a fundamental factor in understanding processes in general,
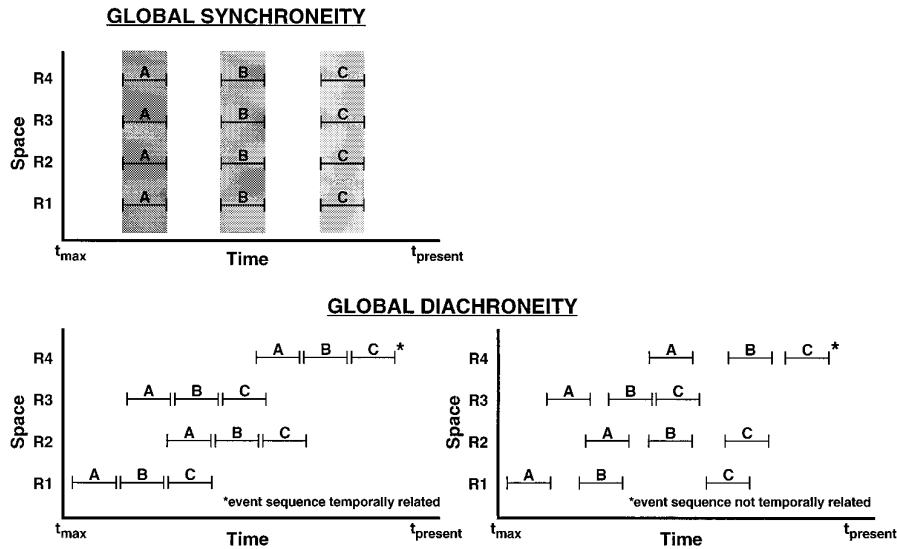
FIG. 7. Idealized models of the surface evolution of Venus. Tmax, age of oldest surface unit; Tpresent, present time. Three arbitrary events (A, B, and C) and four arbitrary regions (R1–R4) illustrate spatial and temporal relations of events. The relative timing of these events—"A" corresponding to the oldest and "C" the youngest—is established by regional mapping (e.g., Basilevsky and Head 1995). In the global synchroneity model, individual events occur globally at the same time. In the global diachroneity model, events occur in the same relative sequence from region to region, but occur at different times. Two versions of global diachroneity are shown: in the model at left, each event is shown to follow immediately the preceding event, implying a temporal relation between events; whereas, it is alternatively possible (model at right) for the time between the events to be variable, or for the events to overlap temporally, implying a lack of temporal relation.

and tectonic processes in particular, that it should not be assumed, but rigorously constrained.

5.3. Does Tessera Formation Require Weak Lithosphere?

Our understanding of venusian rheological and thermal properties is meager (Phillips and Hansen 1994). Lithospheric strength depends on composition, temperature, fluid content, strain rate, thickness, and the strength of individual layers that comprise the lithosphere. Although deformation style can provide an indication of material strength during deformation, because tesserae represent the deformation of the surface layer(s) of Venus their deformation style should not be used as a proxy for lithospheric strength (e.g., Solomon *et al.* 1991, 1992). The overall strength of the lithosphere depends on the strength of its strongest layer, which is not likely the surface layer. The style of tessera deformation may, however, have implications for the relative strength of individual layers that comprise portions of the crust, and for changes in near-surface layer rheology through time.

Because deformation style (e.g., brittle versus ductile) is related to rheology, the character of tessera deformation should provide clues to the surface rheology at the time of local tesserization, as might be the case for the formation of ribbon terrain as discussed above. In addition, the progressive deformation of some tesserae, such as extended folded terrain (ribbon) terrain, might record changes in shallow crustal rheology through time. The observation

that some tesserae host folds (e.g., fold terrain and lava flow pattern tesserae) without obvious faults also indicates that the surface layer(s) involved in these deformations acted plastically, at the scale of observation. Therefore the deformed material either had fractures of all orientations throughout, allowing it to deform plastically (frictional sliding), was viscous as a result of being hot or "wet," deformed at very slow strain rates, or some combination of these factors.

The observation that fold terrain tesserae show little to no obvious strain gradient for 100s of kilometers perpendicular to their structural trends suggests that these tesserae deformed due to stress transmitted from below (shear traction), rather than due to edge, or in plane, forces (e.g., Hansen and Phillips 1995). The transmission of stress from below requires that the material at depth be stronger than the surface layer, to which stress is transmitted. In this case the weak lower crust must be weak enough to allow the upper crust to decouple from the upper mantle, yet strong enough to transmit stress from the upper mantle to the upper crust. Thus the presence of dominantly contractional tesserae might place constraints (in time and/or space) on the rheological layering of the mechanical lithosphere, but it cannot robustly constrain the strength or rheology of the overall mechanical lithosphere.

If tesserae can be *robustly* argued to have formed globally synchronously then, and only then, might the implications of crustal or lithospheric layering be extended to a specific stage of Venus evolution. It is also possible that

tesserae formed diachronously and record local rheological variations, due perhaps to local thermal history or composition. Further structural analysis of tessera terrains aimed at documenting deformation (strain) patterns and histories, and determining how they relate to tectonic processes in time and space, will likely place important constraints on tectonic and geodynamic models.

6. SUMMARY AND CONCLUSIONS

Reconnaissance analysis of selected examples of "tesserae" indicates that not all tesserae were formed by similar processes. The range of spatial and temporal strain patterns and deformation histories recorded by various tessera patches indicates that tesserae should not be considered a single map unit; rather we need to focus on delineating and understanding the temporal and spatial strain patterns in individual tessera patches. Identifying "tesserae" as a single unit for the purpose of local geologic studies is appropriate, depending on the question. For example, Quaternary studies often treat all crystalline and sedimentary rocks as "basement" because the interest is in the more recent Quaternary processes. However, we do not turn to these Quaternary studies to gain a direct understanding of how the crystalline and sedimentary basement evolved and deformed, or to understand the tectonic processes responsible. Similarly, treating much of the deformed crust of Venus as a single map unit—tesserae—does not allow us to frame the proper questions, much less determine valid constraints for models aimed at understanding the tectonic processes responsible for deformation of these various fragments of venusian crust. But if we focus efforts on mapping individual tessera patches and on understanding their structural and kinematic evolution we may be able to understand a great deal about Venus tectonics, and the processes (likely more than one!) of tessera formation.

Accepting that different types of tesserae form in different geologic environments we can make some preliminary proposals about tesserae. Fold and S-C terrain are found only in Ishtar Terra, and thus we consider their style of formation unique, as Ishtar is unique. The observation that lava flow and basin-and-dome terrains reside within the interior of crustal plateaus whereas folded ribbon terrain and extended folded terrain lie within the margins of crustal plateaus certainly places limits on models of crustal plateau formation. The recognition that ribbon terrain records early extension of large tracts of flat, rheologically layered crust is fundamental to models of crustal plateau formation. Coupled with the observation that large inliers also host these types of tesserae, this is suggestive of a model in which large tessera inliers represent old flooded crustal plateaus (e.g., Phillips and Hansen 1994). In crustal plateaus, extended folded (±ribbon) terrain lies within the high-standing topographic margins (e.g., Bindschadler et

al. 1992, Phillips and Hansen 1994), and thus would be the most likely portion to be preserved with "sinking" of crustal plateaus. Graben-dominated tessera inliers may represent the extensional remains of ancient crustal plateaus. In contrast, small inliers marked by densely fractured terrain display evidence of very minor extension. The fracture patterns of these small inliers are similar in size, style, variation, and changes in orientation to the fracture patterns associated with coronae and chasmata (e.g., Stofan et al. 1992, Hamilton and Stofan 1996). It is possible then that these tessera inliers represent flooded (deflated or "sunken") ancient corona–chasma chains such as Parga or Hecate.

Thus it is possible, and remains to be tested, that tesserae could form in several types of tectonic environments, including (1) as a result of subsurface flow in Ishtar Terra, (2) as variable sequences of surface-layer extension and contraction in crustal plateaus, (3) as flooded crustal plateaus which have deflated or sunken, and are preserved as large plains inliers, and (4) as densely fractured surface layers—fractured as a result of corona and chasma formation, likely within a dominantly tensile crustal environment (e.g., Phillips and Hansen 1994)—which have since sunken and become variably flooded, and thus preserved as isolated, scattered, highly fractured inliers. If such models of formation are correct, tesserae would *not* form a global onion skin (e.g., Basilevsky and Head 1995); tesserae would not represent a globally synchronous unit; tesserae would not record a single period of deformation in Venus' tectonic history; nor would a single mechanism for tessera formation suffice. In the same sense that deformed rocks on Earth formed (and continue to form) in a wide variety of tectonic environments, tesserae likely record a range of spatially and temporally discreet tectonic processes. This view of tesserae brings to mind a picture of Venus which is not catastrophic, but rather cyclic or evolutionary. Diapirs rise and form corona/chasma regions, and with time these regions "sink" and become flooded; crustal plateaus form, and with time they "sink" and become flooded. Ishtar Terra, unique on Venus, comprises a region in which mantle residuum collects at depth; the lower crust is thought to thicken as a result of shear forces associated with structurally deeper residuum and displacement of the lower crust results, in turn, in translation and folding of the upper crust which deforms in a rug-like fashion becoming detached from the lower crust (e.g., Hansen and Phillips 1995). Whatever mantle mechanism(s) drive the corona/chasma environment (broad upwelling?) and the crustal plateau environment (also broad upwelling?) could change location through time. This view of Venus and the role of tessera formation in her evolution remains to be tested, but the view broadly fits the available data.

In summary, not all tesserae appear to be created equally, and in order to understand these chapters of

Venus' tectonic story, we must understand the range of tectonic processes represented by their range in deformation histories. Such an understanding will require mapping and analyzing the deformed crust of Venus at the highest detail allowed by the data. High-resolution *Magellan* SAR images and the ability to digitally manipulate these images afford us with an exciting opportunity to begin to unravel the structural evolution of individual deformation provinces, whether they occur in Ishtar Terra, within one of several crustal plateaus, or as individual inliers within the plains. Unraveling local and regional geologic histories will lead to (1) further recognition of different styles of deformation, (2) an understanding of geologic and tectonic histories of individual deformed regions, and (3) the development and testing of local, regional, and global models of causative lithospheric mechanics and tectonic processes.

REFERENCES

ANDERSON, E. M. 1951. *The Dynamics of Faulting.* Oliver and Boyd, Edinburg, Scotland.

BARSUKOV, V. L., A. T. BAZILEVSKII (SIC), R. O. KUZMIN, M. S. MARKOV, V. P. KRYUCHKOV, O. V. NIKOLAEVA, A. A. PRONIN, A. L. SUKHANOV, I. M. CHERNAYA, B. A. BURBA, N. N. BOBINA (SIC), AND V. P. SHASHKINA 1985. Main types of structures of the northern hemisphere of Venus. *Solar System Res.* **19,** 1–9.

BARSUKOV, V. L., A. T. BASILEVSKY, G. A. BURBA, N. N. BOBINNA, V. P. KRYUCHKOV, R. O. KUZMIN, O. V. NIKOLAEVA, A. A. PRONIN, L. B. RONCA, I. M. CHERNAYA, V. P. SHASHKINA, A. V. GARANIN, E. R. KUSHKY, M. S. MARKOV, A. L. SUKHANOV, V. A. KOTELNIKOV, O. N. RZHIGA, G. M. PETROV, Y. N. ALEXANDROV, A. I. SIDORENKO, A. F. BOGOMOLOV, G. I. SKRYPNIK, M. Y. BERGMAN, L. V. KUDRIN, I. M. BOKSHTEIN, M. A. KRONROD, P. A. CHOCHIA, Y. S. TYUFLIN, S. A. KADNICHANSKY, AND E. L. AKIM 1986. The geology and geomorphology of the Venus surface as revealed by the radar images obtained by Veneras 15 and 16. *J. Geophys. Res.* **91,** D378–D398.

BASILEVSKY, A. T., AND J. W. HEAD 1995. Global stratigraphy of Venus: Analysis of a random sample of thirty-six test areas. *Earth, Moon, Planets* **66,** 285–336.

BASILEVSKY, A. T., A. A. PRONIN, L. B. RONCA, V. P. KRYUCHKOV, A. L. SUKHANOV, AND M. S. MARKOV 1986. Styles of tectonic deformations on Venus: Analysis of Venera 15 and 16 data. *J. Geophys. Res.* **91,** D399–D411.

BERTHÉ, D., P. CHOUKROUNE, AND P. JEGOUZO 1979. Orthogneiss, mylonite and noncoaxial deformation of granite: The example of the South Amorican shear zone. *J. Struct. Geol.* **1,** 31–42.

BINDSCHADLER, D. L., AND J. W. HEAD 1989. Characterization of Venera 15/16 geologic units from Pioneer reflectivity and roughness data. *Icarus* **77,** 3–20.

BINDSCHADLER, D. L., AND J. W. HEAD 1991. Tessera terrain, Venus: Characterization and models for origin and evolution. *J. Geophys. Res.* **96,** 5889–5907.

BINDSCHADLER, D. L., A. deCHARON, K. K. BERATAN, S. E. SMREKAR, AND J. W. HEAD 1992a. Magellan observations of Alpha Regio: Implications for formation of complex ridged terrains on Venus. *J. Geophys. Res.* **97,** 13,563–13,577.

BINDSCHADLER, D. L., G. SCHUBERT, AND W. M. KAULA 1992b. Coldspots and hotspots: Global tectonics and mantle dynamic of Venus. *J. Geophys. Res.* **97,** 13,495–13,532.

BINDSCHADLER, D. L., M. A. KREVLAVSKY, M. A. IVANOV, J. W. HEAD, A. T. BASILEVSKY, AND Y. G. SHKURATOV 1990. Distribution of tessera terrain on Venus: Prediction for Magellan. *Geophys. Res. Lett.* **17,** 171–174.

CAMPBELL, D. B., J. W. HEAD, J. K. HARMON, AND A. A. HINE 1983. Venus: Identification of banded terrain in the mountains of Ishtar Terra. *Science* **221,** 644–647.

CHAPMAN, M. G. 1995. Relations between plate movement and Phoebe Regio Tessera? *Lunar Planet. Sci.* **XXVI,** 233.

CORNSINI, M., A. VAUCHEZ, C. ARCHANJO, AND E. F. J. de Sa 1991. Strain transfer at continental scale from a transcurrent shear zone to a tranpressional fold belt: The Patos-Serido system, northeastern Brazil. *Geology* **19,** 586–589.

ENGELDER, T., AND P. GEISER 1980. On the use of regional joint sets as trajectories of paleostress fields during the development of the Appalachian plateau, New York. *J. Geophys. Res.* **85,** 6319–6341.

FARR, T. G. 1993. Radar interaction with geologic surfaces. In *Guide to Magellan Image Interpretation* (J. P. Ford, J. J. Plaut, C. M. Weitz, T. G. Farr, D. A. Senske, E. R. Stofan, G. Michaels, and T. J. Parker, Eds.), pp. 45–56. NASA JPL, Pasadena.

FORD, J. P., R. G. BLOM, J. A. CRISP, C. ELACHI, T. G. FARR, R. S. SAUNDERS, E. E. THEILIG, S. D. WALL, AND S. B. YEWELL 1989. *Spacebourne Radar Observations—A Guide for Magellan Radar-Image Analysis.* NASA Jet Propulsion Laboratory, Pasadena.

GILMORE, M. S., AND J. W. HEAD 1992. Sequential deformation of plains along tessera boundaries on Venus: Evidence from Alpha Regio. *International Colloquium on Venus.* LPI Contribution No. 789, pp. 34–36.

GOLOMBEK, M. P. 1979. Structural analysis of lunar grabens and the shallow crustal structure of the moon. *J. Geophys. Res.* **84,** 4657–4666.

GREEN, J., AND N. M. SHORT 1971. *Volcanic Landforms and Surface Features.* Springer-Verlag, New York.

GRIMM, R. E. 1994. Recent deformation rates on Venus. *J. Geophys. Res.* **99,** 23,163–23,171.

GRIMM, R. E., AND S. C. SOLOMON 1988. Viscous relaxation of impact crater relief on Venus: Constraints on crustal thickness and thermal gradient. *J. Geophys. Res.* **93,** 11,911–11,929.

HAMILTON, V. E., AND E. R. STOFAN 1996. The geomorphology and evolution of Hecate Chasma, Venus. *Icarus,* **121,** 171–194.

HANSEN, V. L. 1992. Regional non-coaxial deformation on Venus: Evidence from western Itzpapalotl Tessera. *Lunar Planet. Sci.* **XXIII,** 478–479.

HANSEN, V. L., AND R. J. PHILLIPS 1995. Formation of Ishtar Terra, Venus: Surface and gravity constraints. *Geology* **23,** 292–296.

HERRICK, R. R. 1994. Resurfacing history of Venus. *Geology* **22,** 703–706.

IVANOV, M. A., AND A. T. BASILEVSKY 1993. Density and morphology of impact craters on tessera terrain, Venus. *Geophys. Res. Lett.* **20,** 2579–2582.

IVANOV, M. A., AND J. W. HEAD 1995. Tessera terrain on Venus: Global distribution and characteristics and implications for the geologic history of Venus. In *Venus II Abstract Booklet.* The University of Arizona, Tucson.

KAULA, W. M., D. L. BINDSCHADLER, R. E. GRIMM, V. L. HANSEN, K. M. ROBERTS, AND S. E. SMREKAR 1992. Styles of deformation in Ishtar Terra and their implications. *J. Geophys. Res.* **97,** 16,085–16,120.

KEEP, M., AND V. L. HANSEN 1994. Structural evolution of Maxwell Montes, Venus: Implications for venusian mountain belt formation. *J. Geophys. Res.* **99,** 26,015–26,028.

LISTER, G. S., AND A. W. SNOKE 1984. S-C mylonites. *J. Struct. Geol.* **6,** 617–638.

McGILL, G. E. 1971. Attitude of fractures bounding straight and arcuate lunar rilles. *Icarus* **14,** 53–58.

PHILLIPS, R. J. 1993. The age spectrum of the venusian surface. *Eos* **74(16),** 187.

PHILLIPS, R. J., AND V. L. HANSEN 1994. Tectonic and magmatic evolution of Venus. *Ann. Rev. Earth Planet. Sci.* **22,** 597–654.

PHILLIPS, R. J., R. F. RAUBERTAS, R. E. ARVIDSON, I. C. SARKAR, R. R. HERRICK, N. IZENBERG, AND R. E. GRIMM 1992. Impact crater distribution and the resurfacing history of Venus. *J. Geophys. Res.* **97,** 15,923–15,948.

POLLARD, D. D., AND A. AYDIN 1988. Progress in understanding jointing over the past century. *Geol. Soc. Am. Bull.* **100,** 1181–1204.

PRICE, M., AND J. SUPPE 1994. Mean age of rifting and volcanism on Venus deduced from impact crater densities. *Nature* **372,** 756–759.

PRICE, N. J., AND J. W. COSGROVE 1990. *Analysis of Geological Structures.* Cambridge Univ. Press, Cambridge, England.

RAMSAY, J. G., AND M. I. HUBER 1983. *The Techniques of Modern Structural Geology, Volume 1: Strain Analysis.* Academic Press, London, England.

RAMSAY, J. G., AND M. I. HUBER 1987. *The Techniques of Modern Structural Geology, Volume 2: Folds and Fractures.* Academic Press, London, England.

SCHABER, G. G., R. G. STROM, H. J. MOORE, L. A. SODERBLOM, R. L. KIRK, D. J. CHADWICK, D. D. DAWSON, L. R. GADDIS, J. M. BOYCE, AND J. RUSSELL 1992. Geology and distribution of impact craters on Venus: What are they telling us? *J. Geophys. Res.* **97,** 13,257–13,301.

SENSKE, D. A., G. G. SCHABER, AND E. R. STOFAN 1992. Regional topographic rises on Venus: Geology of western Eistla Regio and comparison to Beta Regio and Atla Regio. *J. Geophys. Res.* **97,** 13,395–13,420.

SIBSON, R. H. 1984. Fault rocks and fault mechanisms. *J. Geol. Soc. London* **133,** 191–213.

SIMPSON, C., AND S. M. SCHMID 1983. An evaluation of the sense of movement in sheared rocks. *Geol. Soc. Am. Bull.* **94,** 1281–1288.

SMREKAR, S. E., AND S. C. SOLOMON 1992. Gravitational spreading of high terrain in Ishtar Terra, Venus. *J. Geophys. Res.* **97,** 16,121–16,148.

SOLOMON, S. C. 1993a. A tectonic resurfacing model for Venus. *Lunar Planet. Sci.* **XXIV,** 1331–1332.

SOLOMON, S. C. 1993b. The geophysics of Venus. *Phys. Today,* 48–55.

SOLOMON, S. C., J. W. HEAD, W. M. KAULA, D. McKENZIE, B. PARSONS, R. J. PHILLIPS, G. SCHUBERT, AND M. TALWANI 1991. Venus tectonics: Initial analysis from Magellan. *Science* **252,** 297–312.

SOLOMON, S. C., S. E. SMREKAR, D. L. BINDSCHADLER, R. E. GRIMM, W. M. KAULA, G. E. McGILL, R. J. PHILLIPS, R. S. SAUNDERS, G. SCHUBERT, S. W. SQUYRES, AND E. R. STOFAN 1992. Venus tectonics: An overview of Magellan observations. *J. Geophys. Res.* **97,** 13,199–13,255.

SQUYRES, S. W., D. G. JANKOWSKI, M. SIMONS, S. C. SOLOMON, B. H. HAGER, AND G. E. McGILL 1992. Plains tectonism on Venus: The deformation belts of Lavinia Planitia. *J. Geophys. Res.* **97,** 13,579–13,599.

STOFAN, E. R., D. A. SENSKE, AND T. J. PARKER 1993. Tectonic features in Magellan data. In *Guide to Magellan Image Interpretation* (J. P. Ford, J. J. Plaut, C. M. Weitz, T. G. Farr, D. A. Senske, E. R. Stofan, G. Michaels, and T. J. Parker, Eds.), pp. 93–108. NASA JPL, Pasadena.

STOFAN, E. R., V. L. SHARPTON, G. SCHUBERT, G. BAER, D. L. BINDSCHADLER, D. M. JANES, AND S. W. SQUYRES 1992. Global distribution and characteristics of coronae and related features on Venus: Implications for origin and relation to mantle processes. *J. Geophys. Res.* **97,** 13,347–13,378.

STOKES, W. L., AND D. J. VARNE 1955. *Glossary of Selected Geologic Terms, with Special Reference to Their Use in Engineering.* Colorado Scientific Society, Denver.

SUKHANOV, A. L. 1986. Parquet: Regions of areal plastic dislocations. *Geotectonics* **20,** 294–305.

SUKHANOV, A. L. 1987. Parquet on Venus: Areas of regional deformations. *Lunar Planet. Sci.* **XVIII,** 972–973.

TANAKA, K. L., D. A. SENSKE, G. G. SCHABER, AND M. PRICE 1995. The geologic framework of Venus. In *Venus II Abstract Booklet*, pp. 47. The University of Arizona, Tucson.

TWISS, R. J., AND E. M. MOORES 1992. *Structural Geology.* Freeman, New York.

WILLIS, J. J., AND V. L. HANSEN 1995. Caldera-related volcanism and collapse at Ishtar Terra, Venus. *Eos* **76(46),** F341.